Electronic Supplementary Information

Copper Nanoparticles Decorated on Cobalt Oxide Nanosheets Derived from Bimetallic Metal-Organic-Framework for Hydrolysis of Ammonia Borane

Qiuju Wang,[ab] Lianli Zou [ab] and Qiang Xu *[abcd]

[a.] Research Institute of Electrochemical Energy, National Institute of Advanced Industrial Science and Technology (AIST), Ikeda, Osaka 563-8577, Japan.

[b.] Graduate School of Engineering, Kobe University, Nada Ku, Kobe, Hyogo 657-8501, Japan.

[c.] AIST-Kyoto University Chemical Energy Materials Open Innovation Laboratory (ChEM-OIL), National Institute of Advanced Industrial Science and Technology (AIST), Kyoto 606-8501, Japan.

[d.] Department of Chemistry, Southern University of Science and Technology (SUSTech), Xueyuan Ave, Nanshan, Shenzhen, Guangdong 518055, China.

Chemicals

All chemicals were commercially available and used without further purification. 2,5-dihydroxyterephthalic acid (H_4DOBDC, Tokyo Chemical Industry Co., Ltd., ≥98.0%), cobalt(II) acetate 4-hydrate ($Co(CH_3COO)_2{\cdot}4H_2O$, Kishida Chem. Co., 99%), copper(II) acetate 1-hydrate ($Cu(CH_3COO)_2{\cdot}H_2O$, Kishida Chem. Co., 99%), methanol (Kishida Chem. Co., 99.8%), cobalt(II) nitrate hexahydrate ($Co(NO_3)_2{\cdot}6H_2O$, Sigma-Aldrich, ≥98%), copper(II) nitrate, 3-hydrate ($Cu(NO_3)_2{\cdot}3H_2O$, Kishida Chem. Co., 99.5%), N, N-dimethylformamide (DMF, Tokyo Chemical Industry Co., Ltd., 99%), ammonia borane (AB, NH_3BH_3, JSC Aviabor, >97%), ethanol (C_2H_5OH, Kishida Chem. Co., >99.8%), and *n*-hexane (Kishida Chem. Co., 96%) were used as received. De-ionized (DI) water with a specific resistance of 18.2 MΩ·cm was obtained by reverse osmosis followed by ion-exchange and filtration (RFD 250NB, Toyo Seisakusho Kaisha, Ltd., Japan).

Instrumentation and methods

Laboratory powder X-ray diffraction (XRD) patterns were collected for the samples on a Rigaku Ultima IV X-ray diffractometer with Cu Kα source (40 kV, 40 mA). The N_2 adsorption/desorption isotherms were obtained at 77 K using automatic volumetric adsorption equipment (Belsorp-max). The metal contents of the catalyst were analyzed using inductively coupled plasma optical emission spectroscopy (ICP-OES) on Thermo Scientific iCAP6300. XPS spectra were recorded on a Shimadzu ESCA-3400 using an Mg Kα source. Scanning electron microscopy (SEM) analyses were carried out with a scanning electron microscope (JEOL JSMIT100 and Hitachi S-5000). The transmission electron microscopy (TEM) and high-annular dark-field scanning TEM (HAADF-STEM) images were recorded on a Titan3 G2 60-300 (FEI) machine under operating voltages of 300 kV. Element mapping images were obtained on a Titan3 G2 60-300 (FEI).

Elemental analyses were performed on CE EA1110 and Perkinelmer 2400II instruments.

Syntheses of MOFs

(1) Co-MOF-74

50 mL methanol solution of H_4DOBDC (1.5 mmol) was added into 100 mL methanol solution of $Co(CH_3COO)_2{\cdot}4H_2O$ (4 mmol) dropwise with sonication and kept for 2 h. The mixture was centrifuged and washed with fresh methanol for 2 times, and then soaked into fresh methanol for solvent exchange for 3 days. For each day, fresh methanol was changed. At last, the sample was dried in the vacuum oven at 60 °C.

(2) Cu-MOF-74

Cu-MOF-74 was prepared by a similar process like Co-MOF-74 except using $Cu(CH_3COO)_2{\cdot}H_2O$ (2 mmol) instead of $Co(CH_3COO)_2{\cdot}4H_2O$ (4 mmol).

(3) Cu-Co-MOF-74

Cu-Co-MOF-74 was prepared by a similar process like Co-MOF-74 except adding $Cu(CH_3COO)_2{\cdot}H_2O$ (0.08 mmol) into the methanol solution of $Co(CH_3COO)_2{\cdot}4H_2O$ (4 mmol) during the preparation. Cu-Co-MOF-74 with different adding amount of $Cu(CH_3COO)_2{\cdot}H_2O$ (0.04, 0.12, 0.16, 0.20 and 0.24 mmol) were also prepared by the similar process.

(4) Cu-Co-MOF-74-MB

Cu-Co-MOF-74 with micro-scale bulk morphology (designated as Cu-Co-MOF-74-MB) was prepared by solvothermal procedure: 0.75 mmol H_4DOBDC, 2 mmol $Co(NO_3)_2{\cdot}6H_2O$ and 0.04 mmol $Cu(NO_3)_2{\cdot}3H_2O$ were dissolved into a 60 mL mixture of

DMF, ethanol and H_2O with volume ratio of 1:1:1 and stirred for 0.5 h. Then the mixture was transferred into a 100 mL autoclave and heated at 100 °C for 24 h in a programming oven. After that, the mixture was centrifuged and washed by fresh methanol for 2 times, and then soaked into fresh methanol for solvent exchange for 3 days. Fresh methanol was changed for every day. Finally, the sample was dried in the vacuum oven at 60 °C

Syntheses of control samples for AB hydrolysis

(1) Cu-Co-MOF-74-*T* catalysts

Cu-Co-MOF-74 (50 mg) was transferred into a programming furnace and heated to a preset temperature under argon atmosphere (designated as Cu-Co-MOF-74-*T*, *T* stands for calcination temperature (°C), including 200, 350 and 650 °C) with a heating rate of 5 °C/min and kept at the preset temperature for 1 h. After cooling down to RT naturally, the sample was used as the catalyst for AB hydrolysis directly.

(2) Other control samples

a. The as-prepared Co-MOF-74, Cu-MOF-74 and Cu-Co-MOF-74-MB (50 mg) were used as catalysts for AB hydrolysis at 25 ^{o}C for comparation.

b. Cu@Co-MOF-74

Cu@Co-MOF-74 was prepared by the so-called double solvents method (DSM).[1] 50 mg Co-MOF-74 (preheated at 80 °C overnight in the vacuum oven) was dispersed into 50 mL *n*-hexane, and 60 μL aqueous solution of $Cu(CH_3COO)_2 \cdot H_2O$ (n_{Cu} = 0.005 mmol) was added to the dispersion dropwise in 30 min. After stirring for 6 h, the sediment was separated and dried at 80 °C in the vacuum oven overnight. The as-prepared sample was used for AB hydrolysis directly.

c. Metal ions and organic ligands for catalysis

2 mL aqueous solution of $Co(CH_3COO)_2 \cdot 4H_2O$ (0.204 mmol), $Co(CH_3COO)_2 \cdot 4H_2O$

(0.204 mmol)/$Cu(CH_3COO)_2{\cdot}H_2O$ (0.005 mmol), $Cu(CH_3COO)_2{\cdot}H_2O$ (0.005 mmol) and H_4DOBDC(0.102 mmol) were used directly for AB hydrolysis at RT for comparation.

Characterization of catalytic activity

(1) Procedure for AB hydrolysis

Reaction apparatus for measuring the H_2 evolution from AB is the same as previously reported.[2] In general, 2 mL aqueous dispersion of the as-prepared catalyst (original weight of MOF is 50 mg) was placed in 30 mL two-necked round-bottom flask which was placed in a water bath at a preset temperature (25, 30, 40, and 50 °C). A gas burette filled with water was connected to the reaction flask to measure the volume of released gas (temperature kept constant at 298 K during measurement). The reaction started when 1.0 mL of aqueous AB solution (n_{AB} = 1 mmol) was injected into the system using a syringe. The volume of the evolved gas was monitored by recording the displacement of water in the gas burette.

(2) Durability testing of Cu-Co-MOF-74

The durability testing of Cu-Co-MOF-74 was performed at 25 °C. The procedure was the same as described above. For each cycle, 1.0 mL aqueous AB solution (1 mmol) was injected to the catalytic system without further treatment of the catalysts. The experiment was repeated for 5 times.

Calculation methods

The turnover frequency (TOF) reported here is an apparent TOF value based on the total amount of metals ($n = n_{Cu} + n_{Co}$) in the catalyst (according to the ICP results), which is calculated from the equation as follow:

$$TOF = P_0V/(RTnt)$$

Where P_0 is the atmospheric pressure (101325 Pa), V is the final generated volume of gas (H_2), R is the universal gas constant (8.3145 m^3 Pa mol^{-1} K^{-1}), T is the room temperature (298 K), n is total mole number of Co and Cu, and t is the completion time of the reaction subtracted with the in-situ reduction time of catalyst in minute.

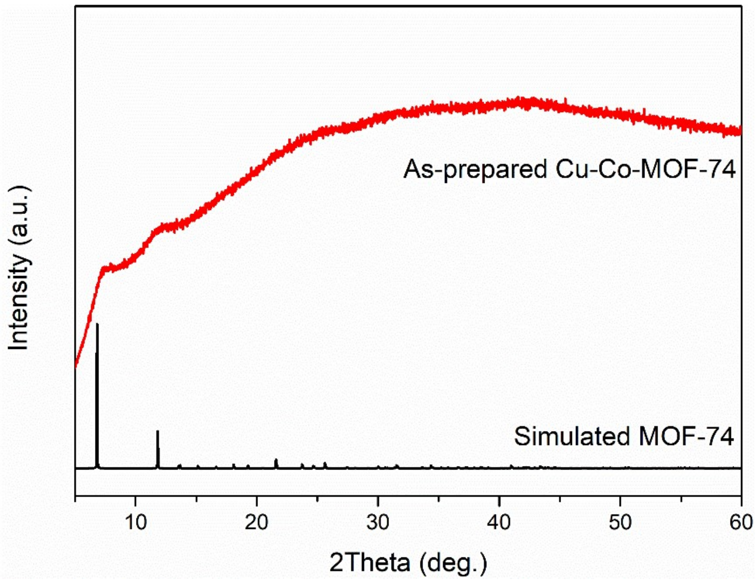

Fig. S1. The XRD patterns of the as-prepared Cu-Co-MOF-74 by the sonication method and the simulated MOF-74.

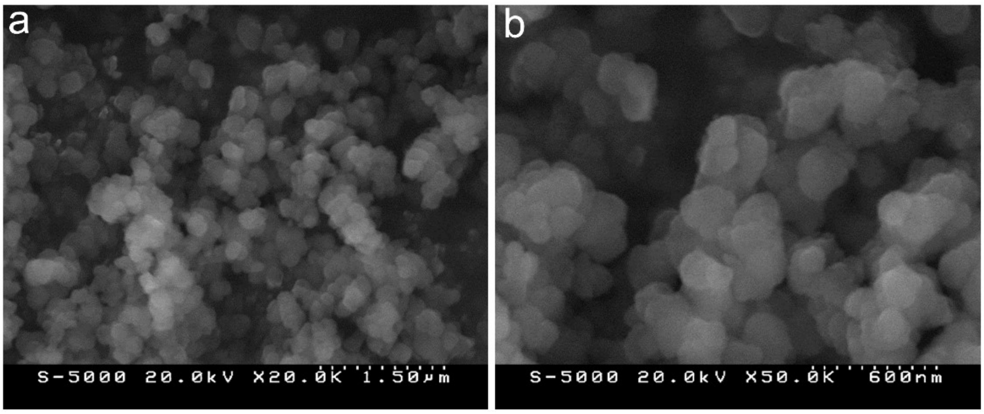

Fig. S2. (a, b) SEM images of Cu-Co-MOF-74.

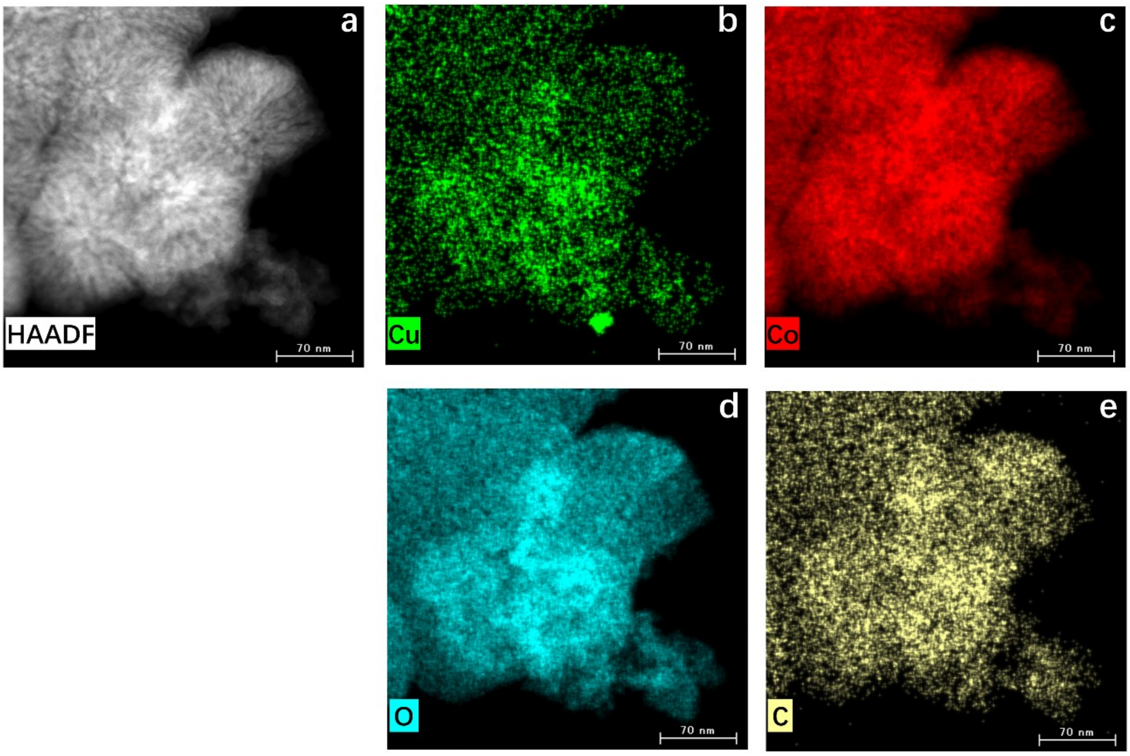

Fig. S3. (a) The HAADF-STEM image of Cu-Co-MOF-74 and its corresponding elemental mapping images of (b) Cu, (c) Co, (d) O and (e) C.

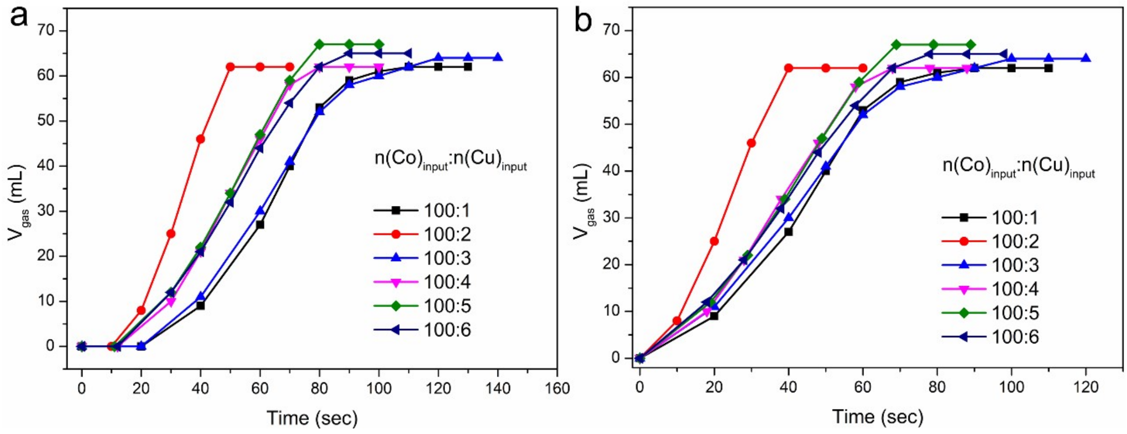

Fig. S4. Gas evolution from aqueous AB by Cu-Co-MOF-74 with different $n(Co)_{input}$:$n(Cu)_{input}$: (a) curves with reduction time of MOF and (b) curves without the reduction time of MOF.

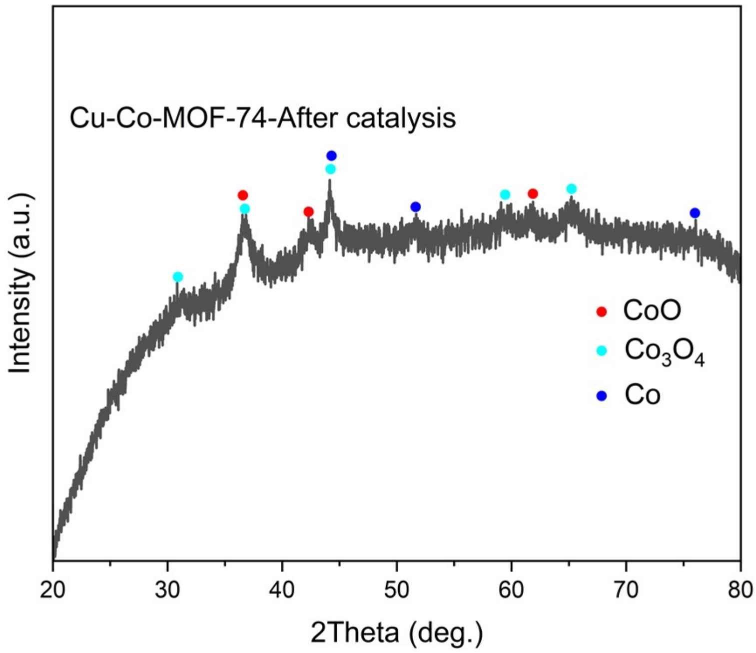

Fig. S5. XRD pattern of Cu-Co-MOF-74 after catalysis of AB hydrolysis for 5 cycles.

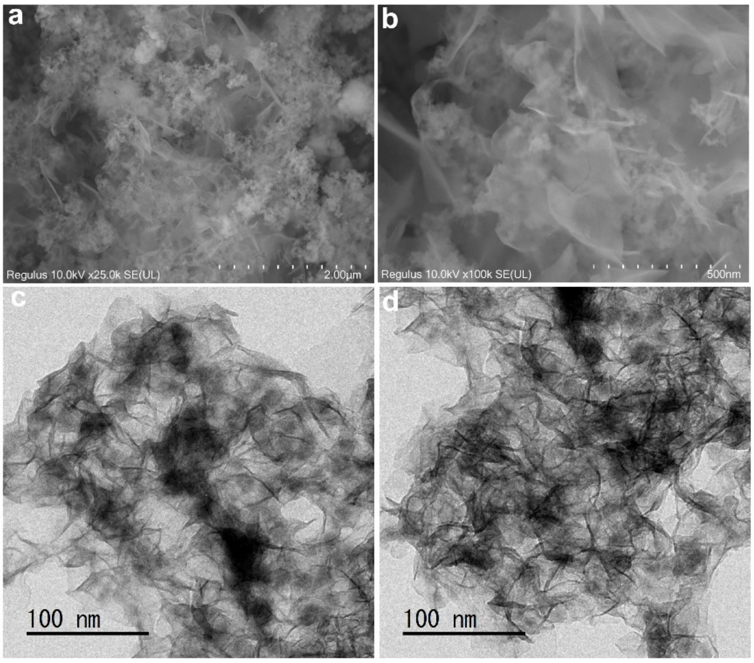

Fig. S6. (a, b) SEM and (c, d) TEM images of Cu-Co-MOF-74 after catalysis of AB hydrolysis.

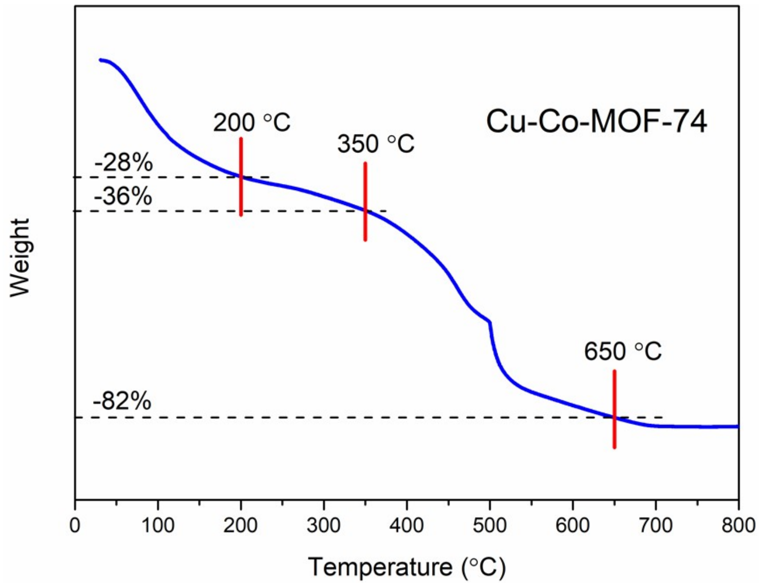

Fig. S7. TG curve for Cu-Co-MOF-74 (with a heating rate of 10 °C/min from RT to 800°C under Ar atmosphere).

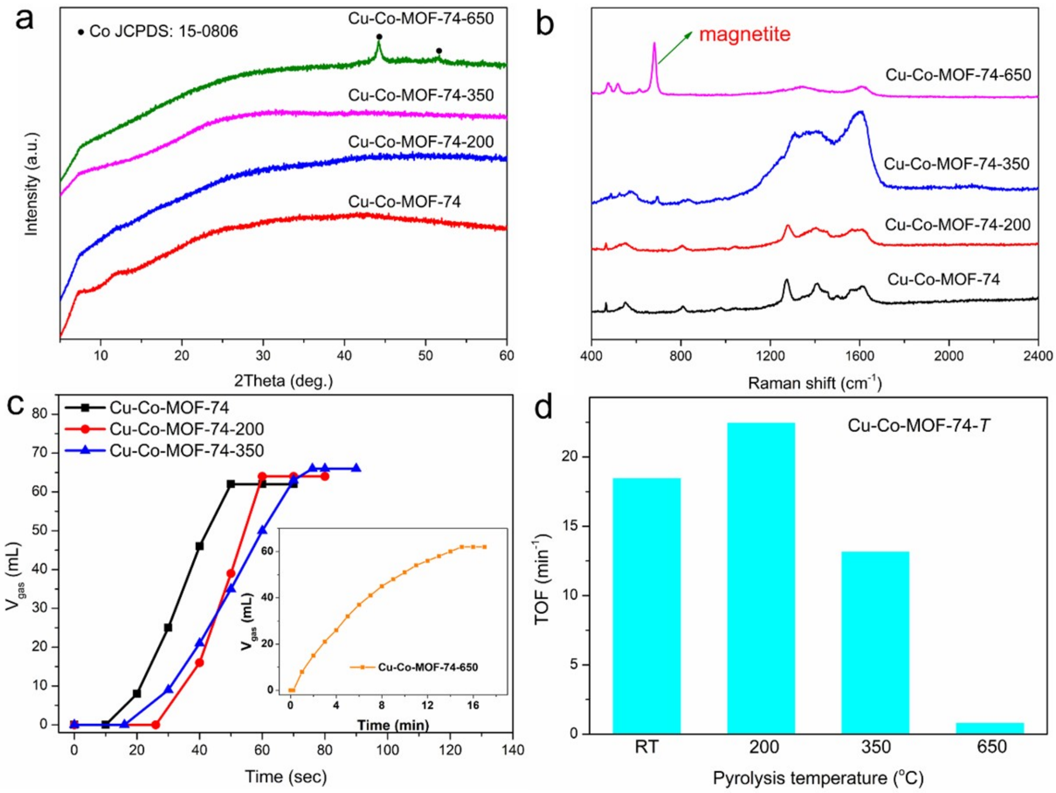

Fig. S8. (a) XRD patterns, (b) Raman spectra, (c) gas evolution from aqueous AB and (d) the corresponding TOF values of Cu-Co-MOF-74-*T* catalysts (25 °C, n_{Co}= 0.204 mmol, n_{Cu}= 0.005 mmol, n_{AB}= 1 mmol).

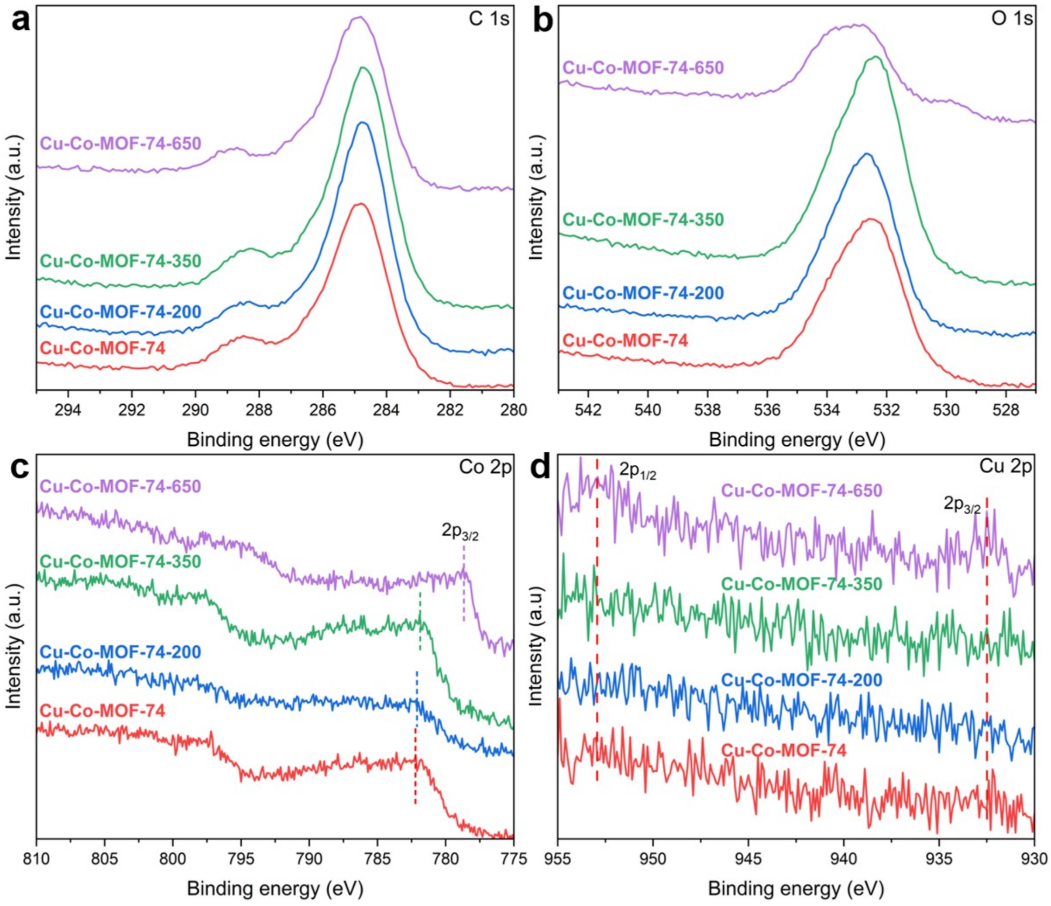

Fig. S9. XPS spectra of (a) C 1s, (b) O 1s, (c) Co 2p and (d) Cu 2p of Cu-Co-MOF-74-*T* catalysts (*T* = RT, 200, 350 and 650 ºC, respectively)

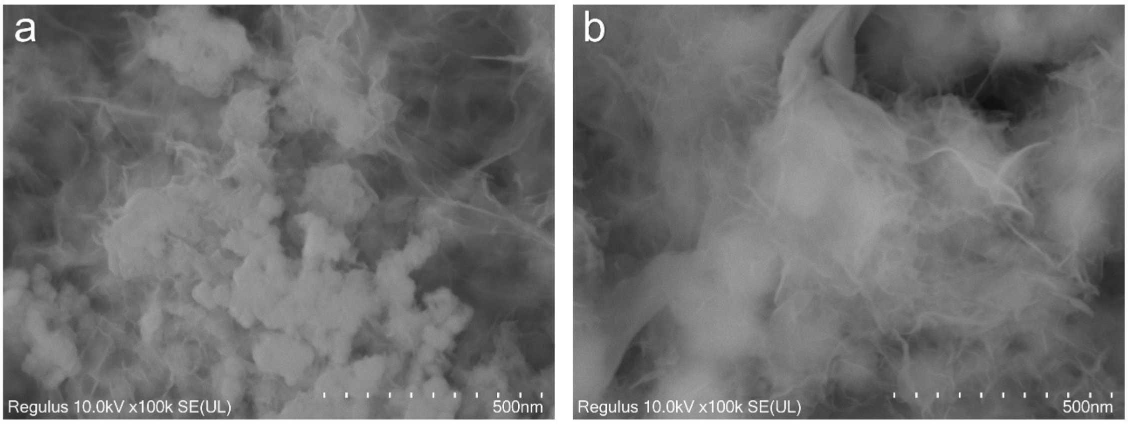

Fig. S10. SEM images of (a) Cu-Co-MOF-74-200 and (b) Cu-Co-MOF-74-350 after using for AB hydrolysis.

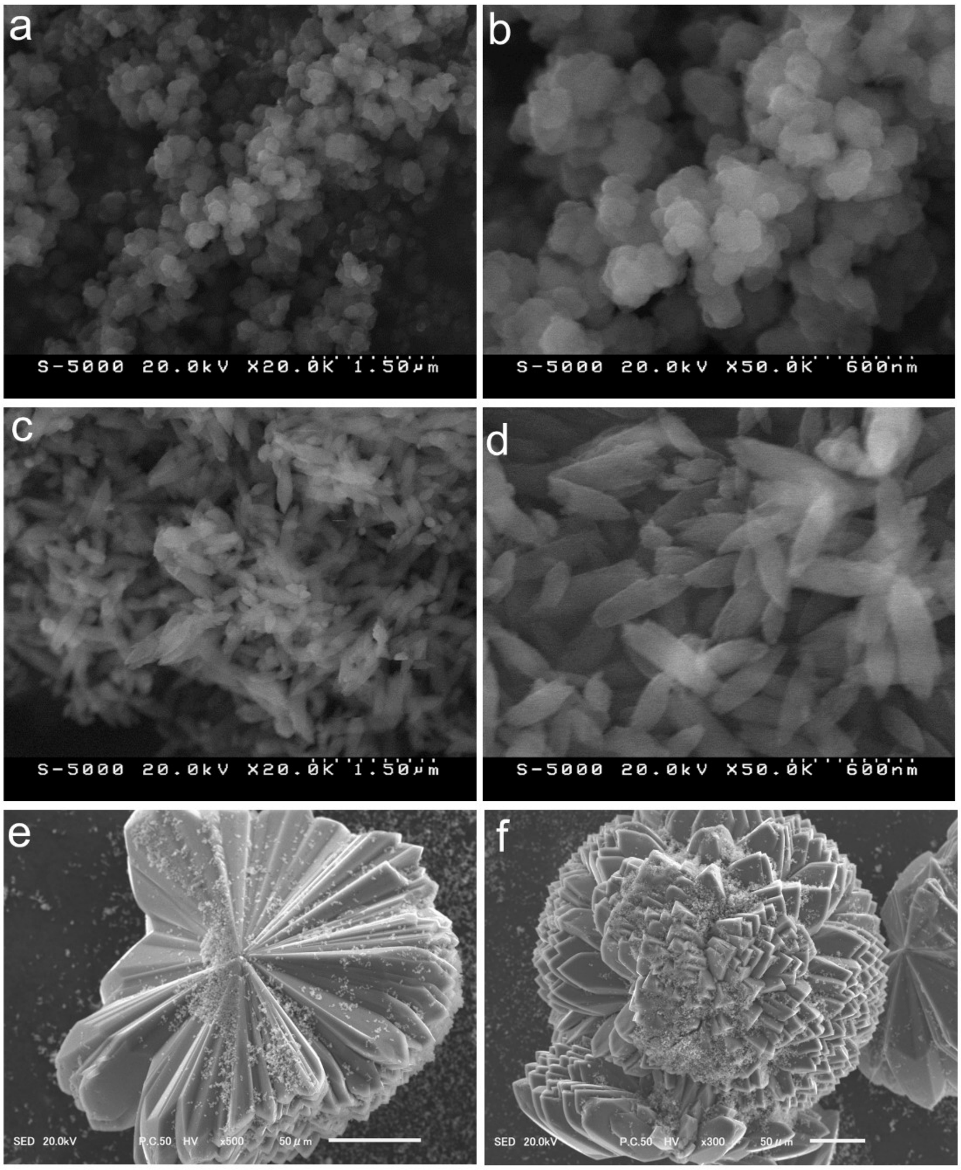

Fig. S11. SEM images of (a, b) Co-MOF-74 and (c, d) Cu-MOF-74 prepared by sonication method at RT, and (e, f) Cu-Co-MOF-74-MB prepared by solvothermal process.

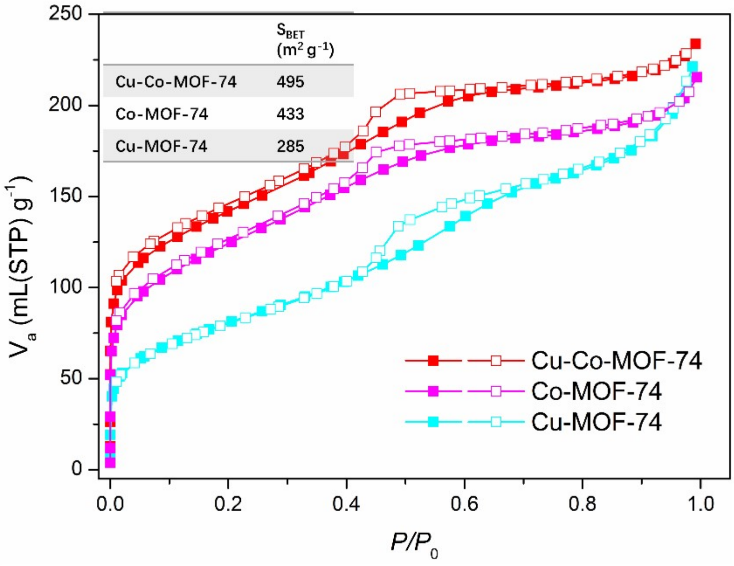

Fig. S12. N_2 sorption isotherms of different MOFs (filled and open symbols represent adsorption and desorption branches, respectively) and the inset is the corresponding BET specific surface areas.

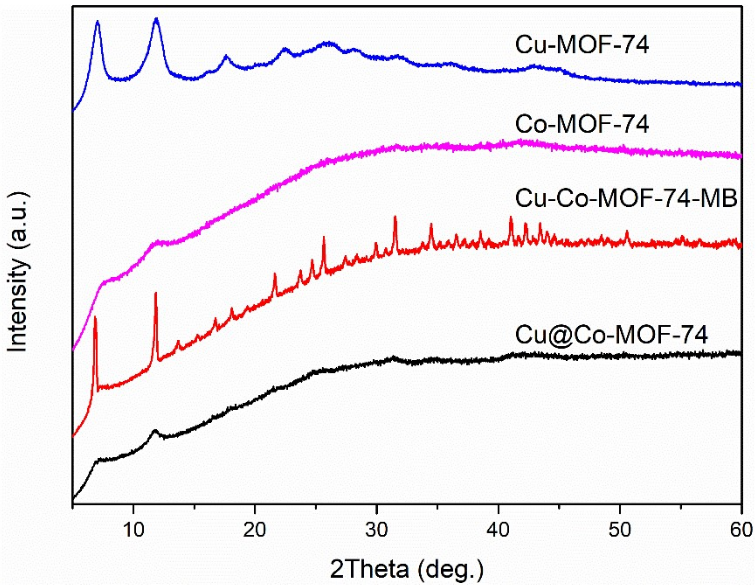

Fig. S13. XRD patterns of control samples: Cu-MOF-74, Co-MOF-74, Cu-Co-MOF-74-MB and Cu@Co-MOF-74.

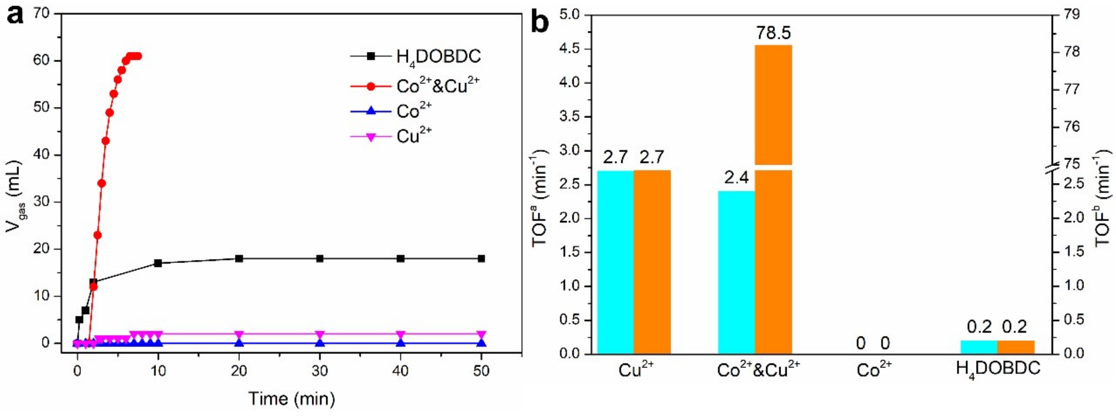

Fig. S14. (a) Gas evolution from aqueous AB and (b) the corresponding TOF values using H_4DOBDC, $Cu(CH_3COO)_2 \cdot H_2O$, $Co(CH_3COO)_2 \cdot 4H_2O$ and the mixture of $Co(CH_3COO)_2 \cdot 4H_2O$ and $Cu(CH_3COO)_2 \cdot H_2O$ as catalysts, respectively (25 °C, n_{AB}= 1 mmol).

**In Fig. S14, blue bars stand for TOF^a (left Y axis) calculated on the input amounts of control samples; orange bars stand for TOF^b (right Y axis), and TOF^b is specially designed for the mixture of Co^{2+} and Cu^{2+}, which is calculated on the amount of only Cu (TOF^a and TOF^b for the other samples are the same).*

Table S1. Catalytic activities of latest Cu-based catalysts for hydrogen generation from ammonia borane.

Catalyst	Temp. (^oC)	Solvent	Addition	TOF (min^{-1})	E_a ($kJ\ mol^{-1}$)	Ref.
Cu@CoO_x	25	H_2O	-	18.5[a]/775[b]	37.4	This work
	30	H_2O	-	22.5[a]/939[b]		
	40	H_2O	-	30.9[a]/1292[b]		
	50	H_2O	-	61.8[a]/2583[b]		
$CuO-NiCo_2O_4$-0.8	25	H_2O	NaOH	23.2	34.2	3
$Co_{40}Cu_{60}$@S16LC-20	30	H_2O	-	16.36	38.1	4
$Cu_{0.5}Ni_{0.5}$/h-BN	30	H_2O	NaOH	6.33	23.02	5
Cu/$Cu_{0.76}Co_{2.24}O_4$	25	H_2O	NaOH	50.33	30.6	6
		H_2O	-	28.12		
$Cu_{0.4}Co_{0.6}$/BNNFs	25	H_2O	-	8.42	21.8	7
Cu@Co@Ni/MOF	25	H_2O	-	31	-	8
Cu/$La_{0.7}Sr_{0.3}CoO_3$	30	H_2O	-	14.05	-	9
$Cu_{0.9}Ni_{0.1}$/*p*-BN	25	MeOH	-	27.1	27.8	10
Cu@Ni_6-MOF	25	H_2O	NaOH	69.1	31.6	11
$Co_{2.4}Cu_{0.6}(PO_4)_2$	25	H_2O	NaOH	72.6	29.0	12

[a] *Corresponding TOF values calculated on the total amount of Cu and Co;*

[b] *Corresponding TOF values calculated on the amount of only Cu.*

References

1. A. Aijaz, A. Karkamkar, Y. J. Choi, N. Tsumori, E. Ronnebro, T. Autrey, H. Shioyama and Q. Xu, *J. Am. Chem. Soc.*, 2012, **134**, 13926-13929.

2. W.-W. Zhan, Q.-L. Zhu, S. Dang, Z. Liu, M. Kitta, K. Suenaga, L.-S. Zheng and Q. Xu, *Small*, 2017, **13**, 1603879.
3. Y. Feng, Y. Li, Q. Liao, W. Zhang, Z. Huang, X. Chen, Y. Shao, H. Dong, Q. Liu and H. Li, *Fuel*, 2023, **332**, 126045.
4. J. R. Deka, D. Saikia, N.-F. Lu, K.-T. Chen, H.-M. Kao and Y.-C. Yang, *Appl. Surf. Sci.*, 2021, **538**, 148091.
5. K. Liu, S. Yang, Y. Chen, W. Zhang, P. Liu and X. Zheng, *Int. J. Hydrogen Energy*, 2022, **47**, 33741-33753.
6. C. Wang, Y. Ren, J. Zhao, S. Sun, X. Du, M. Wang, G. Ma, H. Yu, L. Li, X. Yu, X. Zhang, Z. Lu and X. Yang, *Appl. Catal., B*, 2022, **314**, 121494.
7. X. Yang, Q. Li, L. Li, J. Lin, X. Yang, C. Yu, Z. Liu, Y. Fang, Y. Huang and C. Tang, *J. Power Sources*, 2019, **431**, 135-143.
8. J.-L. Sun, Y.-Z. Chen, B.-D. Ge, J.-H. Li and G.-M. Wang, *ACS Appl. Mater. Inter.*, 2019, **11**, 940-947.
9. D. Salinas-Torres, M. Navlani-García, Y. Kuwahara, K. Mori and H. Yamashita, *Catal. Today*, 2020, **351**, 6-11.
10. P. Li, H. Liu, C. Wang, Y. Fang, Z. Guo, J. Lin, Y. Huang, C. Yu, L. Hu, C. Tang and Z. Liu, *ChemistrySelect*, 2023, **8**, e202204413.
11. W. Xu, M. Liu, S. Wang, Z. Peng, R. Shen and B. Li, *Int. J. Hydrogen Energy*, 2022, **47**, 23213-23220.
12. Y. Feng, Y. Zhu, Y. Li, L. Li, F. Lv, Z. Li, H. Li and M. He, *Int. J. Hydrogen Energy*, 2020, **45**, 17444-17452.